Systematic Self-Interference Mitigation in Full Duplex Antenna Arrays Via Transmit Beamforming

2023 International Conference on Electromagnetics in Advanced Applications (ICEAA) | 979-8-3503-2058-9/23/$31.00 ©2023 IEEE | DOI: 10.1109/ICEAA57318.2023.10297706

Systematic Self-Interference Mitigation In Full Duplex Antenna Arrays Via Transmit Beamforming

1st Mustafa Ayebe
Electrical Engineering Department (E2)
Chalmers University of Technology
Göteborg, Sweden
ayebe@chalmers.se

2nd Johan Malmström
Surveillance
SAAB
Järfälla, Sweden
johan.malmstrom@saabgroup.com

3rd Sten E. Gunnarson
Surveillance
SAAB
Järfälla, Sweden
sten.gunnarsson@saabgroup.com

4th Henrik Holter
Hardware Research
Ericsson AB
Stockholm, Sweden
henrik.holter@ericsson.com

5th Marianna Ivashina
Electrical Engineering Department (E2)
Chalmers University of Technology
Göteborg, Sweden
marianna.ivashina@chalmers.se

6th Carlo Bencivenni
Electrical Engineering Department
Gapwaves AB
Göteborg, Sweden
carlo.bencivenni@gapwaves.com

7th Rob Maaskant
Electrical Engineering Department (E2)
Chalmers University of Technology
Göteborg, Sweden
rob.maaskant@chalmers.se

***Abstract*—The optimal antenna array excitation vector is derived that maximizes the (realized) array gain in a particular direction while preventing the coupled input power to the low-noise amplifiers on the receive side to exceed a certain maximum threshold level. This is very useful for in-band full-duplex systems where the hardware complexity for self-interference cancellation must be minimized. In this approach, the perfect nulling of interference on the RX side is not required, sparing degrees of freedom for the TX beamformer. We evaluate the performance of the proposed TX beamforming algorithm by showing numerical results of the 25 x-polarized TX and 25 RX with 0.5λ element spacing and λ gap distance between the TX and RX sub-array.**

***Index Terms*—In-band full-duplex, Self-Interference Mitigation, Transmit Beamforming**

I. Introduction

In-band full-duplex (IBFD) is a type of network architecture that allows for simultaneous transmission and reception of signals at the same frequency band and offers the potential to increase the spectrum efficiency and data rate of wireless communication systems as well as improved sensitivity in e.g., radar and Electronic Warfare applications [1]. However, implementing IBFD systems presents a significant challenge due to self-interference (SI) — the transmission of the signal from the transmitter (TX) leaking into the receiver (RX), which needs to be properly mitigated in order to receive the desired signal with maximum spurious free dynamic range. SI can be mitigated consecutively over three domains, namely, the analog-circuit domain, the digital domain, and the propagation domain. The survey in [2] offers a comprehensive collection of these techniques and discusses typical implementation solutions for each of these domains. The analog-circuit domain approaches intend to generate a copy of the transmit signal in order to cancel the SI at the receiver input. The digital domain cancellation exploits the known transmitted data symbols and the estimated SI channel to cancel the residual SI in the digital baseband. The propagation domain methods aim to isolate the transmitter and receiver to reduce the SI arriving at the receiver. These techniques can be categorized into passive and active SI cancellation. Passive SIC techniques are used to electromagnetically isolate the transmitter and receiver. Active SI cancellation techniques are usually applied in the digital and analog domains to exploit the knowledge of its own transmitted signal to cancel the SI, i.e., to generate a cancellation signal in the receive signal path to null the SI.

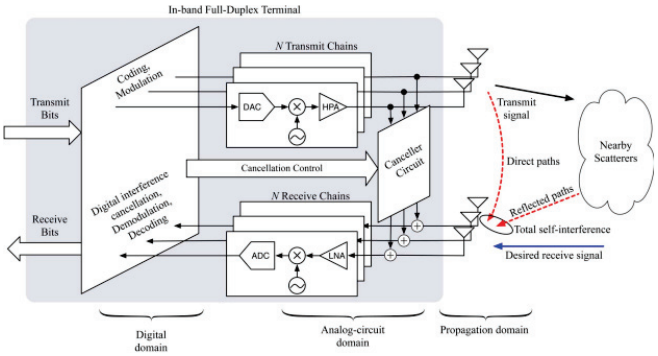

Fig. 1. Block diagram of a typical full-duplex system with three stages of SI cancellation (see the original Fig. 4 in [1]).

Fig. 1 demonstrates that the IBFD terminal accepts a coded

and modulated transmit bitstream in the digital domain, which generates a digital baseband signal for each TX antenna. These digital signals are transformed into analog signals using a digital-to-analog converter (DAC) and are then amplified through a high-power amplifier (HPA) and radiated using a TX antenna. However, this process can introduce some non-idealities into the TX signal, like DAC quantization noise, oscillator phase noise, and amplifier distortion, which result in slight discrepancies between the actual and intended to TX signals.

At the same time, the IBFD terminal functions as an RX over the same frequency band. Each RX antenna receives a signal that is processed through a hardware chain consisting of a low-noise amplifier (LNA), downconverter, and analog-to-digital converter (ADC). The resulting digital baseband signals are jointly processed in the digital domain (which involves demodulation, interference cancellation, and bit decoding) to produce the received bitstream.

In multiple-input multiple-output architectures, digital domain approaches can be used to mitigate the SI on the RX side [3]. With enough isolation between separate and closely positioned TX and RX antenna arrays, an IBFD system could simultaneously transmit and receive in-band. SoftNull [3] is proposed to use TX digital beamforming to reduce self-interference between TX and RX. However, this study does not involve the analysis of the coupling path characteristics between different elements or different sub-array. For large array systems, after using this method, there may still be high SI remaining on some receiver units. The maximum input power for preventing nonlinear gain compression of low noise amplifiers connected to RX antenna elements is generally not considered. Simply relying on nulling the interferer signal at the receiver inputs is a too stringent constraint; Aiming for perfect nulling is undesired as additional hardware cancellation circuitry and/or larger TX antenna arrays increase the hardware complexity and overall cost. Joint TX and RX beamforming aims to minimize the interference below the receiver noise floor, often achieved through an iterative BF approach, which is slow when performed in real-time [2].

To overcome these problems, we propose a novel TX beamforming method that

- Prevents the RF input power to low-noise amplifiers on the RX side to exceed a certain threshold level. To this end, we identify and utilize a subset of TX excitation vectors to achieve this goal
- Performs maximum (realized) gain beamforming using this down-selected set of excitation vectors

This two-stage beamforming method is systematic and non-iterative in nature and is thus believed to have minimal impact on system latency. In fact, the TX-RX communication overhead is comparable with standard channel estimation techniques where knowledge of the TX-RX coupling matrix needs to be obtained. Furthermore, achieving isolation through beamforming relaxes the requirements on the remaining SI cancellation techniques, thereby reducing the overall hardware complexity.

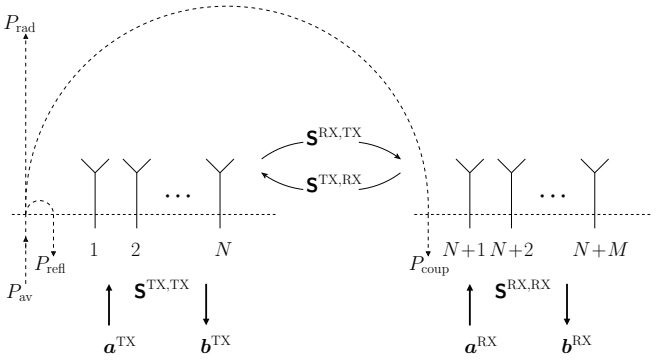

Fig. 2. S-parameter model of full-duplex TX-RX array.

This paper is organized as follows. In Sec. II the problem is formulated and the solution strategy is described. The numerical results are described in Sec. III, after which conclusions are drawn in Sec. IV.

II. Array Model and Definitions

Consider the N-element transmit (TX) antenna array and the M-element receive (RX) antenna array in Fig. 2.

Antenna element $i \in \{1, 2, \ldots, N+M\}$ is assumed to be terminated by Z_i. The antenna port voltage is V_i and the antenna input current I_i. Using the power wave definitions in [4], the incident a_i and reflected b_i power wave amplitudes are defined as

$$a_i = \frac{V_i + Z_i I_i}{2\sqrt{|\mathfrak{Re}\{Z_i\}|}}; \qquad b_i = \frac{V_i - Z_i^* I_i}{2\sqrt{|\mathfrak{Re}\{Z_i\}|}} \tag{1}$$

Accordingly, the vector of TX incident power waves can be expressed as $\boldsymbol{a}^{\text{TX}} = [a_1^{\text{TX}}, a_1^{\text{TX}}, \ldots, a_N^{\text{TX}}]^T$, where ^{T} denotes the transposition operator. Likewise, we can introduce the $N \times 1$ vector of TX reflected power waves as $\boldsymbol{b}^{\text{TX}}$, the $M \times 1$ vector of RX incident power waves as $\boldsymbol{a}^{\text{RX}}$ and the $M \times 1$ vector of RX reflected power waves as $\boldsymbol{b}^{\text{RX}}$. These power waves are related through the antenna S-parameters as

$$\underbrace{\begin{bmatrix}\boldsymbol{b}^{\text{TX}}\\ \boldsymbol{b}^{\text{RX}}\end{bmatrix}}_{\boldsymbol{b}} = \underbrace{\begin{bmatrix}\mathbf{S}^{\text{TX,TX}} & \mathbf{S}^{\text{TX,RX}}\\ \mathbf{S}^{\text{RX,TX}} & \mathbf{S}^{\text{RX,RX}}\end{bmatrix}}_{\mathbf{S}} \underbrace{\begin{bmatrix}\boldsymbol{a}^{\text{TX}}\\ \boldsymbol{a}^{\text{RX}}\end{bmatrix}}_{\boldsymbol{a}} \tag{2}$$

When the TX array is transmitting, and $\boldsymbol{a}^{\text{RX}} = \mathbf{0}$ (matched terminated RX elements), we can define the following powers (*cf.* also Fig. 2):

$$P_{\text{av}} = \frac{1}{2}\sum_{n=1}^{N} \left|a_n^{\text{TX}}\right|^2 = \frac{1}{2}\left(\boldsymbol{a}^{\text{TX}}\right)^H \boldsymbol{a}^{\text{TX}} \tag{3a}$$

$$P_{\text{coup}} = \frac{1}{2}\sum_{m=1}^{M} \left|b_m^{\text{RX}}\right|^2 = \frac{1}{2}\left(\boldsymbol{b}^{\text{RX}}\right)^H \boldsymbol{b}^{\text{RX}} \tag{3b}$$

where ^{H} denotes the Hermitian (conjugate-transpose).

A. Maximum Gain Beamformer

In this section, our objective is to find the optimal excitation vector $\boldsymbol{a}^{\mathrm{TX}}$ that maximizes the (realized) antenna array gain $G^{\mathrm{TX}}(\hat{\boldsymbol{r}})$ in a specific direction $\hat{\boldsymbol{r}}$. The realized antenna array gain is defined as

$$G^{\mathrm{TX}}(\hat{\boldsymbol{r}}) = 4\pi \frac{\frac{1}{2\eta}\left|\boldsymbol{G}^{\mathrm{TX}}(\hat{\boldsymbol{r}})\right|^2}{P_{\mathrm{av}}} \tag{4}$$

where the far-field function $\boldsymbol{G}^{\mathrm{TX}} = r\boldsymbol{E}(\boldsymbol{r})e^{jkr}$ is related to the radiated E-field $\boldsymbol{E}(\boldsymbol{r})$ at the far-field observation point $\boldsymbol{r}$, where $r = |\boldsymbol{r}|$ is the distance from the origin to the far-field observation point. The antenna array far-field function is a linear combination of N antenna embedded element far-field functions $\{\boldsymbol{G}_n^{\mathrm{TX}}\}_{n=1}^N$, i.e.,

$$\boldsymbol{G}^{\mathrm{TX}} = \sum_{n=1}^{N} a_n^{\mathrm{TX}} \boldsymbol{G}_n^{\mathrm{TX}} = \mathbf{G}^{\mathrm{TX}} \boldsymbol{a}^{\mathrm{TX}} \tag{5}$$

where the column-augmented matrix

$$\mathbf{G}^{\mathrm{TX}} = \left[\boldsymbol{G}_1^{\mathrm{TX}}, \boldsymbol{G}_2^{\mathrm{TX}}, \ldots, \boldsymbol{G}_N^{\mathrm{TX}}\right] \tag{6}$$

and where $\boldsymbol{G}_n^{\mathrm{TX}}$ is obtained by exciting element n by an incident wave with unit amplitude while all other elements are terminated in their characteristic impedance. Using (5), the realized array gain in (4) along with (3a) can then be expressed as

$$G^{\mathrm{TX}} = \frac{4\pi}{\eta} \frac{\left(\boldsymbol{a}^{\mathrm{TX}}\right)^H \left(\mathbf{G}^{\mathrm{TX}}\right)^H \mathbf{G}^{\mathrm{TX}} \boldsymbol{a}^{\mathrm{TX}}}{\left(\boldsymbol{a}^{\mathrm{TX}}\right)^H \boldsymbol{a}^{\mathrm{TX}}} \tag{7}$$

Clearly, the realized array gain depends on the excitation vector $\boldsymbol{a}^{\mathrm{TX}}$. The maximum of G^{TX} is found by setting

$$\boldsymbol{\nabla}_{(\boldsymbol{a}^{\mathrm{TX}})^H} G^{\mathrm{TX}} = 0 \tag{8}$$

leading to the generalized eigenvalue equation

$$\left(\mathbf{G}^{\mathrm{TX}}\right)^H \mathbf{G}^{\mathrm{TX}} \boldsymbol{a}^{\mathrm{TX}} = \frac{\left[\left(\boldsymbol{a}^{\mathrm{TX}}\right)^H \left(\mathbf{G}^{\mathrm{TX}}\right)^H \mathbf{G}^{\mathrm{TX}} \boldsymbol{a}^{\mathrm{TX}}\right]}{\left[\left(\boldsymbol{a}^{\mathrm{TX}}\right)^H \boldsymbol{a}^{\mathrm{TX}}\right]} \boldsymbol{a}^{\mathrm{TX}} \tag{9}$$

or simply,

$$\left(\mathbf{G}^{\mathrm{TX}}\right)^H \mathbf{G}^{\mathrm{TX}} \boldsymbol{a}^{\mathrm{TX}} = G^{\mathrm{TX}} \boldsymbol{a}^{\mathrm{TX}} \tag{10}$$

The optimal array excitation that leads to the maximum realized array gain G^{TX} is found by finding the eigenvector of $\left(\mathbf{G}^{\mathrm{TX}}\right)^H \mathbf{G}^{\mathrm{TX}}$ with the largest eigenvalue. Maximizing the gain in this way is well known, see for instance [5, Sec. 10.3].

B. Minimum TX-RX Isolation Constraint

With the power definitions given above, the *total* TX-RX isolation can be expressed as

$$\mathrm{ISO} = \frac{P_{\mathrm{av}}}{P_{\mathrm{coup}}} = \frac{\left(\boldsymbol{a}^{\mathrm{TX}}\right)^H \boldsymbol{a}^{\mathrm{TX}}}{\left(\boldsymbol{b}^{\mathrm{RX}}\right)^H \boldsymbol{b}^{\mathrm{RX}}} \tag{11}$$

where $\boldsymbol{b}^{\mathrm{RX}} = \mathbf{S}^{\mathrm{RX,TX}} \boldsymbol{a}^{\mathrm{TX}}$, hence,

$$\mathrm{ISO} = \frac{\left(\boldsymbol{a}^{\mathrm{TX}}\right)^H \boldsymbol{a}^{\mathrm{TX}}}{\left(\boldsymbol{a}^{\mathrm{TX}}\right)^H \left(\mathbf{S}^{\mathrm{RX,TX}}\right)^H \mathbf{S}^{\mathrm{RX,TX}} \boldsymbol{a}^{\mathrm{TX}}} \tag{12}$$

Eq. (12) can be maximized by requiring that

$$\boldsymbol{\nabla}_{(\boldsymbol{a}^{\mathrm{TX}})^H} \mathrm{ISO} = 0 \tag{13}$$

leading to

$$\boldsymbol{a}^{\mathrm{TX}} = \frac{\left[\left(\boldsymbol{a}^{\mathrm{TX}}\right)^H \boldsymbol{a}^{\mathrm{TX}}\right]}{\left[\left(\boldsymbol{a}^{\mathrm{TX}}\right)^H \left(\mathbf{S}^{\mathrm{RX,TX}}\right)^H \mathbf{S}^{\mathrm{RX,TX}} \boldsymbol{a}^{\mathrm{TX}}\right]} \left(\mathbf{S}^{\mathrm{RX,TX}}\right)^H \mathbf{S}^{\mathrm{RX,TX}} \boldsymbol{a}^{\mathrm{TX}} \tag{14}$$

where one recognizes the isolation function (12), so that

$$\boldsymbol{a}^{\mathrm{TX}} = \mathrm{ISO} \left(\mathbf{S}^{\mathrm{RX,TX}}\right)^H \mathbf{S}^{\mathrm{RX,TX}} \boldsymbol{a}^{\mathrm{TX}} \tag{15}$$

which is a generalized eigenvalue problem of the form

$$\mathbf{A}\boldsymbol{v}_n = \lambda_n \mathbf{B}\boldsymbol{v}_n \tag{16}$$

where the real-valued non-negative eigenvalue λ_n of the n-th eigenvector $\boldsymbol{v}_n$ is given as

$$\lambda_n = \mathrm{ISO} \tag{17}$$

and $\mathbf{A} = \mathbf{I}$ is the identity matrix, and $\mathbf{B} = \left(\mathbf{S}^{\mathrm{RX,TX}}\right)^H \mathbf{S}^{\mathrm{RX,TX}}$. Hence, maximizing ISO in Eq. (12) is done by finding the largest eigenvalue of (16). If the eigenvalues are ordered as $\lambda_1 \geq \lambda_2 \geq \ldots \geq \lambda_P$, where $P = \min(\{N, M\})$, then the principal eigenvector $\boldsymbol{a}^{\mathrm{TX}} = \boldsymbol{v}_1$ maximizes ISO. Likewise, the eigenvector $\boldsymbol{a}^{\mathrm{TX}} = \boldsymbol{v}_P$ corresponding to the smallest eigenvalue λ_P that minimizes ISO. In conclusion,

$$\max \mathrm{ISO} = \mathrm{ISO}(\boldsymbol{v}_1) \qquad \text{or} \qquad \min \mathrm{ISO} = \mathrm{ISO}(\boldsymbol{v}_P) \tag{18}$$

Besides finding the maximum (or minimum) TX-RX isolation level, we can require that

$$\mathrm{ISO}(\boldsymbol{a}^{\mathrm{TX}}) \geq \kappa \tag{19}$$

where κ defines the minimum TX-RX isolation level. To find the subspace of excitation vectors $\boldsymbol{a}^{\mathrm{TX}}$ that satisfies (19), κ is used as a threshold on the singular value spectrum. In other words, if $\{\lambda_n\}_{n=1}^K \geq \kappa$ are the K eigenvalues equal or exceeding the threshold κ, then $\boldsymbol{a}^{\mathrm{TX}}$ can be found in the subspace defined by

$$\boldsymbol{a}^{\mathrm{TX}} \in \mathrm{span}(\{\boldsymbol{v}_1^{\mathrm{TX}}, \boldsymbol{v}_1^{\mathrm{TX}}, \ldots, \boldsymbol{v}_K^{\mathrm{TX}}\}) \tag{20}$$

That is, $\boldsymbol{a}^{\mathrm{TX}}$ can be expressed as a linear combination of the first K eigenvectors:

$$\boldsymbol{a}^{\mathrm{TX}} = \sum_{n=1}^{K} \alpha_n^{\mathrm{TX}} \boldsymbol{v}_n^{\mathrm{TX}} = \mathbf{V}^{\mathrm{TX}} \boldsymbol{\alpha}^{\mathrm{TX}} \tag{21}$$

where the column-augmented matrix

$$\mathbf{V}^{\mathrm{TX}} = \left[\boldsymbol{v}_1^{\mathrm{TX}}, \boldsymbol{v}_2^{\mathrm{TX}}, \ldots, \boldsymbol{v}_K^{\mathrm{TX}}\right] \tag{22}$$

and where the weights $\{\alpha_n^{\mathrm{TX}}\}$ can be chosen freely, for example, to maximize the array gain (see Sec. II-A).

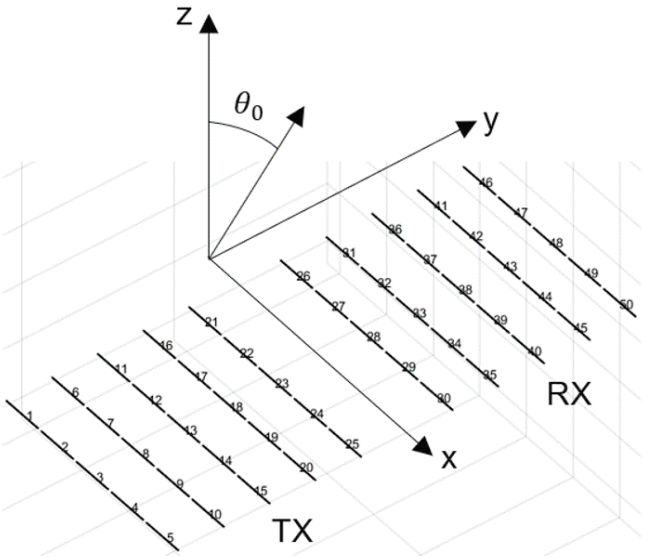

Fig. 3. TX-RX array antenna configuration

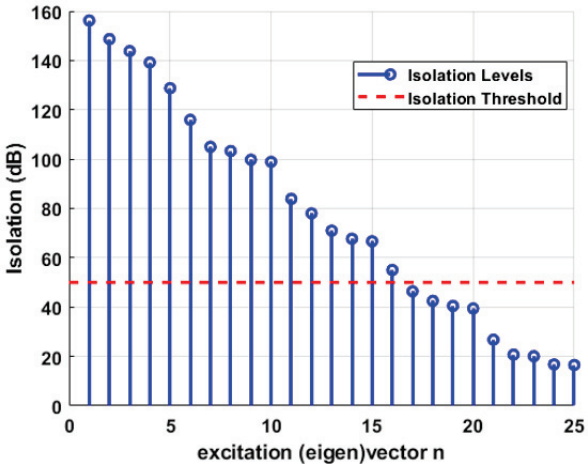

Fig. 4. The eigenvalue spectrum of the isolation matrix.

C. Min. TX-RX Isolation + Max. TX Gain Constraints

The goal is to maximize the realized TX array antenna gain in a particular direction while attaining the total coupled TX-to-RX power below a maximum threshold level, i.e.,

$$\begin{array}{ll} \text{maximize} & G^{\text{TX}}(\boldsymbol{a}^{\text{TX}}) \\ \text{subject to} & \text{ISO}(\boldsymbol{a}^{\text{TX}}) \geq \kappa \end{array} \tag{23}$$

This problem can be solved by first satisfying the isolation constraint, as done in Sec. II-B. That is, we find the subspace of excitation vectors that provides this minimum isolation level κ. In (20), this subspace is spanned by the eigenvectors $\{\boldsymbol{v}_n^{\text{TX}}\}$, so the final excitation vector is a linear combination of eigenvectors using the weights $\{\alpha_n^{\text{TX}}\}$. These weights are chosen to e.g. achieve maximum array gain. We know that, irrespective of these weights, the isolation constraint will be automatically satisfied. To maximize the array gain, we substitute (21) in (10), to yield

$$\left(\mathbf{G}^{\text{TX}}\right)^H \mathbf{G}^{\text{TX}}\mathbf{V}^{\text{TX}}\boldsymbol{\alpha}^{\text{TX}} = G^{\text{TX}}\mathbf{V}^{\text{TX}}\boldsymbol{\alpha}^{\text{TX}} \tag{24}$$

Once again, the largest gain G^{TX} is found by finding the largest eigenvalue of (24) and the corresponding eigenvector is the optimal excitation vector $\boldsymbol{\alpha}^{\text{TX}} = \boldsymbol{\alpha}_{\text{opt}}^{\text{TX}}$. Once $\boldsymbol{\alpha}_{\text{opt}}^{\text{TX}}$ is known, then the optimal array excitation is found to be

$$\boldsymbol{a}_{\text{opt}}^{\text{TX}} = \mathbf{V}^{\text{TX}}\boldsymbol{\alpha}_{\text{opt}}^{\text{TX}} \tag{25}$$

which is the solution to the problem defined in (23).

III. Performance Evaluation

The TX beamforming algorithm is evaluated by considering 25 TX and 25 RX 0.49λ-long x-polarized dipole antenna elements with 0.5λ element spacing and λ gap between sub-arrays, see Fig. 3. The antenna arrays are located $\lambda/4$ above an infinitely large perfect electrically conducting ground plane which is placed on the xy-plane. The H- and E-plane are defined as the yz- and xz-planes, respectively. An in-house MoM code (CAESAR [6]) is used in combination with MATLAB for beamforming.

For demonstration purposes, an arbitrary minimum isolation level is considered 50 dB. The eigenvalue spectrum of $[(\mathbf{S}^{\text{RX,TX}})^H\mathbf{S}^{\text{RX,TX}}]^{-1}$ is presented in Fig. 4. A linear combination of the 16 eigenvectors whose eigenvalue magnitudes exceed the 50 dB specified threshold level can now be used as excitation vectors for further TX beamforming. Fig. 5 shows the element and total TX-RX realized isolation in the H-plane. It can be mathematically proven that the element isolation is always higher than the intrinsic array isolation. This means that the minimum requirement on the total isolation can be set equal to the minimum element isolation. If the actual element isolation turns out higher, the total isolation level can be reduced until one of the element isolations drop below the specified element isolation threshold. However, in this paper we restrict our analysis to a non-iterative approach for the total isolation.

As shown in Fig. 5, the total TX-RX realized isolation is about 20–40 dB without any isolation constraint (=intrinsic isolation). Furthermore, the isolation exceeds the 50 dB threshold value when the minimum TX-RX isolation constraint is enforced. The element isolation is seen to be always higher than that.

Fig. 6 presents the eigenvector far-field patterns for both the largest and smallest eigenvalues which are illustrated in Fig. 4. As can be seen, small power is seen to radiate towards the RX array [top of Fig. 6(a)], which is to be expected when exciting the TX array by the principal eigenvector. However, the eigenvector pattern for the smallest eigenvalue couples more power to the RX array as can be seen by the 'hot spot' at the top of Fig. 6(b).

Fig. 7 shows the maximum realized TX antenna gain as a function of scan angle; the red curve is calculated from an optimal linear combination of the eigenvectors that give at

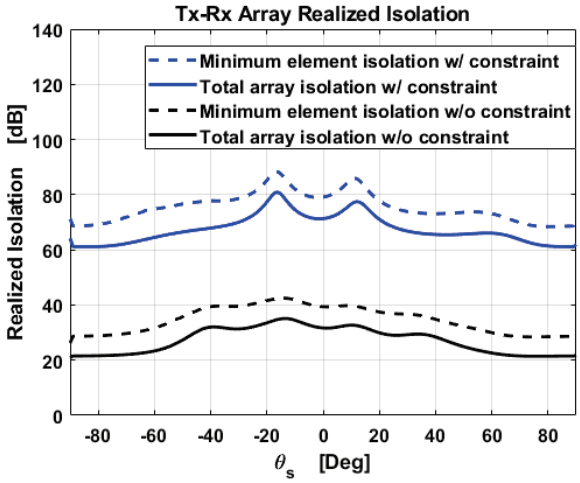

Fig. 5. TX-RX array realized isolation (H-plane)

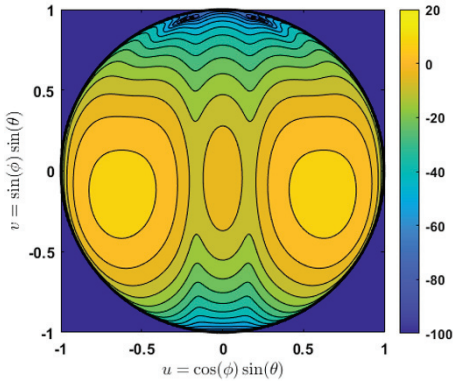

(a)

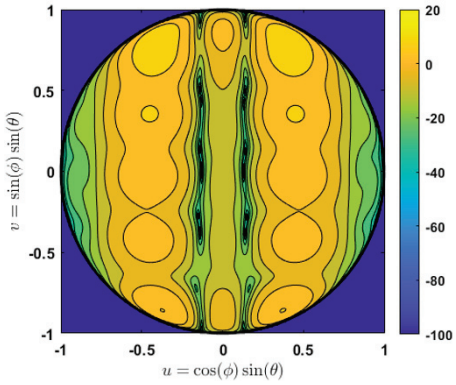

(b)

Fig. 6. (a) The eigenvector pattern for maximum isolation; (b) The eigenvector pattern for minimum isolation

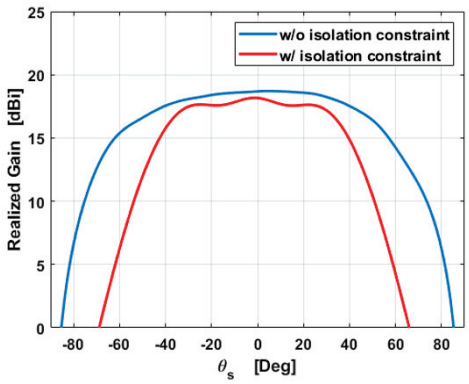

Fig. 7. Maximized realized TX array antenna gain in the H-plane

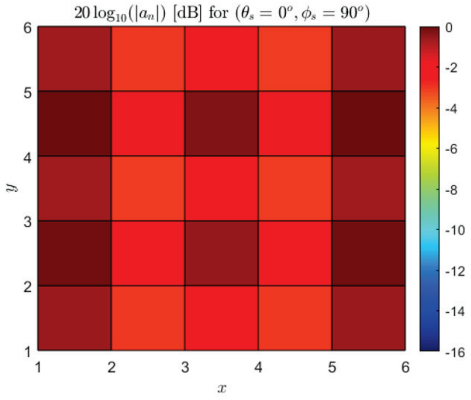

(a)

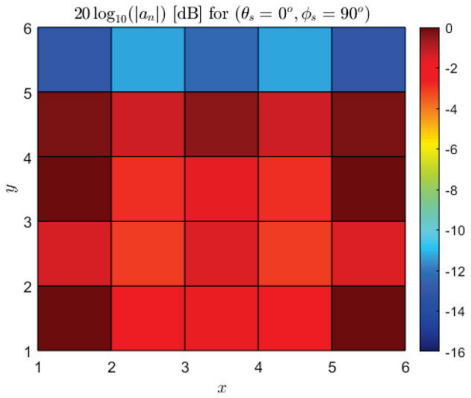

(b)

Fig. 8. The amplitude of the port excitation map for the broadside scan (a) without isolation constraint; (b) with isolation constraint

least 50 dB of isolation. The realized TX array antenna gain pattern becomes worse at large angles due to fewer usable excitation vectors. For example, there is a 5 dB loss at $45°$.

The map of excitation magnitudes in Fig. 8 illustrates that attaining broadside maximum gain does not imply a uniform excitation of the array elements. This is because the embedded element patterns in the matrix $\mathbf{G}^{\mathrm{TX}}$ in Eq. (5) are different due to mutual coupling effects. Furthermore, we sacrifice the elements which are close to the RX array to achieve a minimum isolation level, which is an intuitive result.

IV. Conclusion

The proposed TX beamforming approach is based on finding the TX excitation vector that maximizes the realized array antenna gain in a particular direction subject to keeping the total coupled TX-to-RX self-interference power below a maximum threshold level. In this approach, the perfect nulling of interference on the RX side is not required, sparing degrees of freedom for the TX beamformer.

This approach: (i) ensures that the total power coupled to the RX elements remains below a predetermined threshold to prevent nonlinear gain compression of the LNAs; (ii) retains adequate degrees of freedom for useful TX beamforming without having to rely on increasing array sizes or complex self-interference cancellation networks; (iii) is systematic and achieves optimal excitation and beamformer weight vectors without requiring any iterations once the TX-RX coupling matrix and propagation channels are estimated, which can be done using standard channel estimation techniques commonly used in the wireless communication community.

The final isolation level that can be reached depends on the knowledge on the TX-RX array coupling matrix as well as the dynamic range of DACs and ADCs, which are topics for future research.

Acknowledgment

This research has been carried out in the Gigahertz-ChaseOn Bridge Center in the REMU project financed by Ericsson, SAAB, Gapwaves, Kongsberg, UMS, and Chalmers.

References

[1] A. Sabharwal, P. Schniter, D. Guo, D. W. Bliss, S. Rangarajan and R. Wichman, "In-Band Full-Duplex Wireless: Challenges and Opportunities," in IEEE Journal on Selected Areas in Communications, vol. 32, no. 9, pp. 1637-1652, Sept. 2014.

[2] K. E. Kolodziej, B. T. Perry and J. S. Herd, "In-Band Full-Duplex Technology: Techniques and Systems Survey," in IEEE Transactions on Microwave Theory and Techniques, vol. 67, no. 7, pp. 3025-3041, July 2019.

[3] E. Everett et al., "SoftNull: Many-Antenna Full-Duplex Wireless via Digital Beamforming," IEEE Trans. Wireless Commun., vol. 15, no. 12, Dec. 2016, pp. 8077–92.

[4] K. Kurokawa, "Power waves and the scattering matrix," IEEE Transactions on Microwave Theory and Techniques, vol. 13, no. 2, pp. 194–202, 1965.

[5] R. F. Harrington, Field computation by moment methods. Oxford University Press, Inc., 1996.

[6] R. Maaskant, "Analysis of large antenna systems," PhD Thesis, 2010.